Gurtner, Alex and Boles, Wageeh W. and Walker, Rodney A. (2007) Vibration Compensation for Fisheye Lenses in UAV Applications. In *Proceedings Digital Image Computing: Techniques and Applications (DICTA) 2007*, pages pp. 218-225, Adelaide, Australia.

Vibration Compensation for Fisheye Lenses in UAV Applications

Alex Gurtner[1], A/Prof Rodney Walker[2], A/Prof Wageeh Boles[3]
[1,2,3]*Australian Research Centre for Aerospace Automation (ARCAA)*
Queensland University of Technology (QUT), Brisbane, Australia

Abstract

Low-cost aerial vision systems need to face the challenges of using low quality products to perform aerial photography. Such systems are widely used in remote controlled aircrafts and unmanned aerial vehicles (UAVs) to collect aerial imagery and are used for image acquisition, terrain mapping or remote sensing. A one-pixel shift in a 0.8 mega pixel resolution image captured from a UAV operating at 1000ft will correspond to about 2.5m measurement error on the ground. In our case, a vibrating fisheye lens moving relative to the camera added new uncertainties in the collected images and required compensation. This paper presents a vibration compensation approach using a modified Hough Transform utilizing the circle shaped image provided by a fisheye lens. We define the fisheye circle boundary by using a Canny edge detector. Our vibration compensation was tested using our collected aerial images with enhanced performance in more than 80% of the cases.

1. Introduction

This research is investigating the integration of fisheye lenses and cost effective camera systems onboard unmanned aerial vehicles (UAVs) for terrain mapping applications. One of the most significant challenges facing the practical application of camera systems onboard a UAV or any other dynamic vision system, is compensating for the reduction in image quality due to lens vibrations. This is in addition to the many other challenges in the practical application of camera systems including: varying illumination, sun glare or compensating for the motions of the dynamic platform.

Camera systems onboard aircrafts, such as UAVs, are subject to highly dynamic vibrations from a range of sources. Mechanical (e.g. the engine) and aerodynamic (e.g. aerodynamic forces) sources of vibration cause a significant degradation in the quality of the captured images and, in turn, the suitability of camera systems to a wide range of applications. For example: Vibration causing only a one-pixel shift in a fisheye image captured by a UAV operating at an altitude of 1000 ft above the ground would result in a displacement of approximately 2.5 m, using a 0.8 mega pixel resolution camera. This is additional to all other uncertainties, as they were described in Gurtner et al. [1].

Ertürk et al. [2] stated that image stabilization may remove all of the detected global motion, but is not desired and would remove intentional movements as well. This may be applicable for image stabilization in consumer cameras, but the vibration mentioned in this paper has to be removed completely. The image stabilization presented by Ramachandran and Chellappa [3] uses a three step approach, among others a FFT transform to estimate the rough alignment of image sequences. However, the presented problem in this paper is different and doesn't try to estimate vibrations. To estimate the vibration, we have to detect or track the motion. The only feature remaining stable over time in our images, is the fisheye circle boundary. An interesting method was introduced by Schuster and Katsaggelos [4]. They used a one step approach to detect circles in noisy images. This paper doesn't follow this approach, because of two reasons: First, we want to have separated edge detection from the circle detection, which modularizes the implementation. Second, the paper doesn't consider detecting unknown circle sizes. Another method to detect circle shaped features in image processing applications is the Hough Transform (Kerbyson, Russ, Gonzales and Woods, Jähne [5-8]), which was chosen and modified to suit this application.

A comparison of edge detection algorithms was presented by Shin et al. [9] which concludes that the Canny edge detector performs best under unknown threshold conditions.

0-7695-3067-2/07 $25.00 © 2007 IEEE
DOI 10.1109/DICTA.2007.79

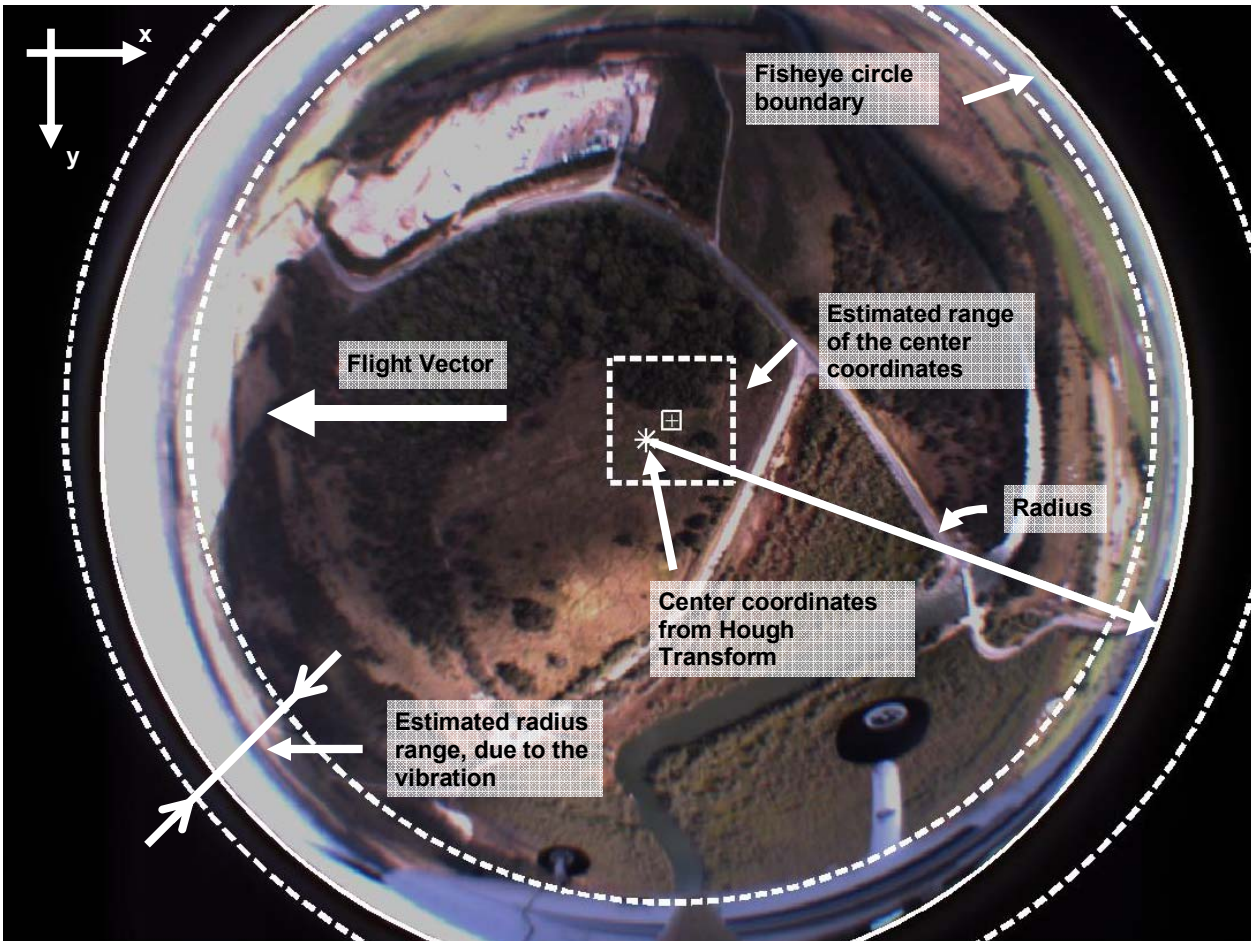

Figure 1: Fisheye image illustration

This paper investigates the development of software algorithms for vibration compensation caused by a vibrating fisheye lens in a moving aircraft. The first section analyses in detail the characteristics of the vibration in the collected images sequences and discusses the conducted flight test. It points out the problem and feature that could be used to detect the vibration. Section 3 discusses the implementation of the two-staged vibration estimation algorithm using a Canny edge detection and a Hough Transform. Experimental results and a discussion about the performance and limitations of the proposed approach are provided in sections 4 and 5.

2. Detailed Analysis of the Fisheye Images

Figure 1 provides an example image of a fisheye image taken during the flight test. The fisheye circle boundary is the circle-line between the black background and the circular fisheye image scene. The flight vector, as indicated in Figure 1, is from right to the left in the image.

Due to the vibration, the coordinates of the fisheye image center and the radius of the fisheye circle boundary aren't accurately known and are estimated instead. In Figure 1, the estimated range of the center coordinates is marked with a dashed square and the range of the radius with two dashed circle lines. The estimated center is marked with a cross in a square, where the center of the circle found with the Hough Transform is marked with a star only. A solid line from the star shows the corresponding radius.

The vibration of the lens was detected after an airborne data collection campaign for UAV research. The data collection included a downward looking camera with a fisheye lens (Point Grey Research Flea camera and Fujinon YV2.2x1.4A-2 fisheye lens), mounted underneath the wing of a Cessna 172 aircraft (Figure 2). Pictures were captured for research purposes, with synchronized GPS and inertial sensor data. The vibration was along x- and y-axis, as

illustrated in Figure 2 and corresponds to the axes drawn into Figure 1.

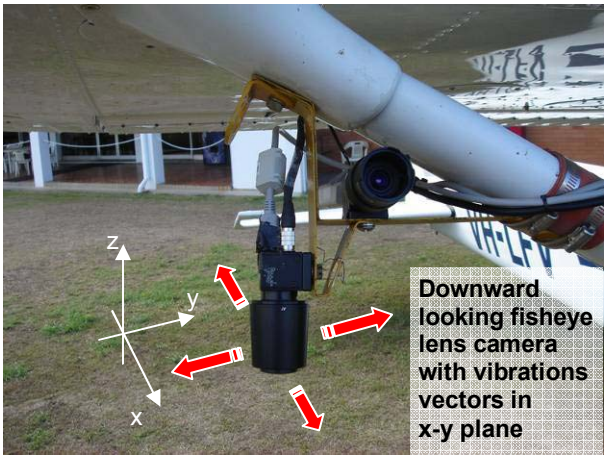

Figure 2: Fisheye lens camera installation

A non-interference fit (clearance in the housing) between the lens housing and the lens is assumed to be the cause of this vibration, which is illustrated in Figure 3 with the arrows.

The vibration significantly decreases the quality of the images and needs to be compensated for further processing in terrain mapping applications.

It is very likely, that this vibration was introduced from wind turbulence (the camera-lens system was directly exposed to the wind) or any other vibrations of the aircraft (e. g. vibrations from engine). A vibration of the lens is not unusual for a low-cost camera-lens system. This research addresses exactly those issues, introduced from low-cost, low quality system components.

The next section has a closer look into the vibration and how it appears on the images and Section 2.2 considers other factors that can decrease the quality of compensating the vibration.

2.1 Description of the Vibration

The vibration can be seen easily by looking at image sequences and monitoring the fisheye circle boundary (see Figure 1). The detected vibration is a movement of the fisheye circle boundary on the image plane, which comes from a movement of the lens relative to the camera, as illustrated in Figure 3 and Figure 4.

Testing the lens in the laboratory showed a translational vibration only, as illustrated in Figure 4. Image sequences of an object in a fixed position relative to the camera, captured while the lens is vibrating relative to the camera show no movement in the center of the lens, but increasing movements towards the fisheye circle boundary, caused by the shifted distortion function of the fisheye lens. On the other hand, rotational vibration would appear as movements (more precise distortions) all over the image scene.

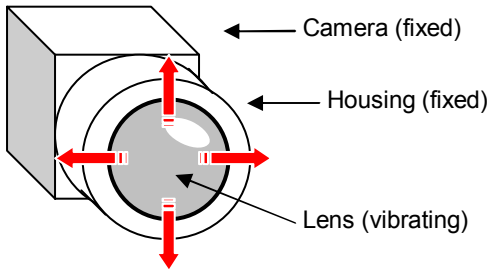

Figure 3: Cause of the lens vibration

The magnitude of the detected vibration can be measured manually by taking a sequence of images with only minor illumination and attitude changes between them. The images are converted to black and white with a constant threshold. The position of the transition from white to black on the fisheye circle boundary is then taken at selected points. The largest translational movement detected was ±5 pixels measured form randomly selected images.

For further processing, the vibration is therefore assumed to be translational, random and limited to ±10 pixels, to cover possible larger movements.

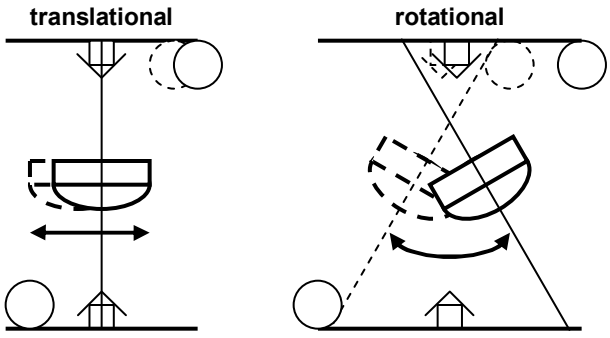

Figure 4: Lens vibration types

2.2 Other Factors Influencing the Fisheye Image Boundary

As mentioned before, there are more factors playing into this problem. These are illumination, sun glare or the effects a climbing, descending and turning aircraft.

Illumination adds errors to the edge detection, so that it can increase or decrease the radius of the fisheye circle. It is also possible, that it shifts the circle for a

certain amount towards one side of the lens or influences the edge detection.

Therefore, it is important to use a circle like matching pattern (such as the Hough Transform for circles), to cover shifts into all directions. An example of the effect of illumination is given in Figure 5, where it expands one side of the circle and would result in errors. However, the flight was conducted during the time where the sun reached its zenith, which minimized this influence.

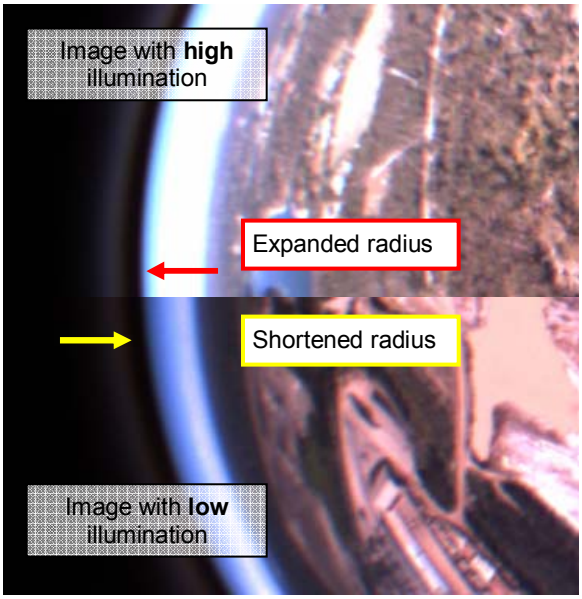

Figure 5: Illumination influence

Sun glare are sun reflections (or direct sunlight) captured in the images, such as from water, roof or car surfaces. An example of sun glare creating a white line over the fisheye image is shown in Figure 6. The white line is of high intensity and expands the fisheye image boundary and therefore influences the edge detection. Sun glare can be detected quite easily and such areas (or the entire image) can be removed from the sequences of images used for further processing.

A climbing, descending or turning aircraft doesn't directly affect the fisheye image circle itself, but it may disturb the edge detection result. Figure 7 shows an example of a climbing aircraft, where the horizon merges together with the fisheye circle boundary. The edge detection failed in separating horizon and the boundary from each other. The edge detection may capture wrong edges or fail completely. Images containing forest, mountains or high buildings can cause major problems.

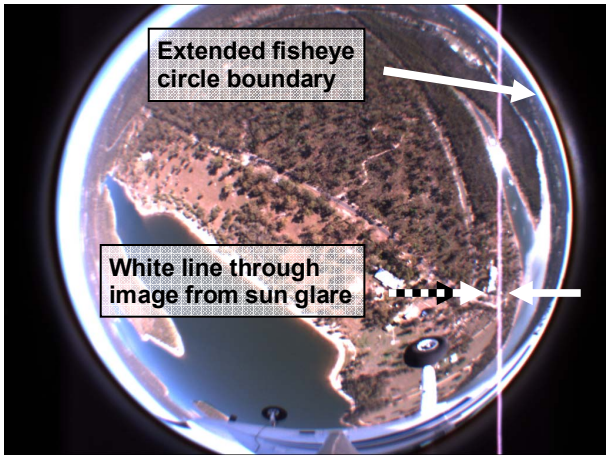

Figure 6: Sun glare drawing a white line

Figure 7: Edge detection distraction

The conclusions out of these disturbances are, that the uncertainty increases over water (due to sun glare and higher illumination of the picture) and during the time the aircraft is making turns. Due to the fact that this research is using a fisheye lens to perform mapping even during turns of the aircraft, these disturbances play a significant role in contributing to the uncertainties in terrain mapping applications and can't be ignored.

3. Vibration Compensation

The vibration compensation depends on image processing techniques alone, since no other information of the vibration was collected. The background and the image scene can't be used to detect the translational motion (vibration), as mentioned before.

The compensation includes the steps of detecting the fisheye image boundary, measuring the movement and removing it.

The following sections present the implementation of the vibration compensation. The first section describes the approach to the problem. Sections 3.2 and 3.3 describe how the vibration compensation was implemented in details.

3.1. Overview of the Approach

By testing different methods to detect the motion of the boundary, it was found that the method has to make use of the circle shape of the image boundary. The method either needs to have a circle like shape detector or it has to work with opposite points in the circle. Having a circle shaped detector will average illumination influences.

Using the Hough Transform performed the best results, where methods like measuring pixel displacement of opposite boundary pixels and phase correlation failed. The Hough Transform is primarily less affected by noise, introduced from a non-circular fisheye boundary, but it requires additional steps in interpreting the results. It is common, that the edge detector detects a lot of misleading edge pixels (>25%) with a divergence of more than 2 pixels compared to a perfect circle. Some areas also need to be removed before applying the Hough Transform, as shown in Figure 8. Especially the upper most circle edges (marked with two parallelograms) show an increased divergence from a perfect circle. Further parts of image have to be removed (marked with rectangles), such as the parts of the image showing the aircraft, which would only introduce more false pixel positions. The remaining image points for the circle detection are marked with dotted lines. In section 4, we present the details of how these circle points are selected.

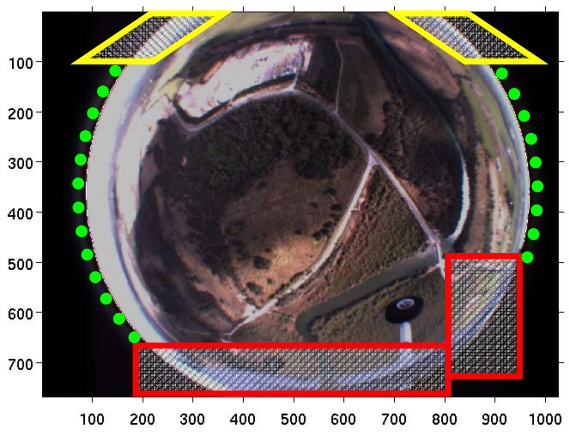

Figure 8: Removed areas in the fisheye images from the circle detection

3.2 Fisheye Circle Boundary Edge Detection

This section presents which color spaces were used for the edge detector and it describes in details of the implementation of the edge detection.

Randomly selected fisheye images were analyzed in the RGB and HSV color spaces. It was found a higher contrast in the fisheye circle boundary area in the RGB-red color plane and the HSV-value color plane. The HSV-value plane increases reflections, where they are weaker in the RGB-red plane. Other HSV color spaces don't show any improvements for the boundary selection and therefore the RGB color space is used for the fisheye circle boundary detection.

The fisheye circle boundary detection uses mainly three steps to achieve a reliable outcome: A Canny edge detection, a grayscale to black and white conversion and removal of the un-useful image parts. The edge detection works in a parallel process. The parallel processes are the Canny edge detection and the limitation to the maximum fisheye circle boundary expansion. At the end, both results are combined.

MATLAB's implementation of the Canny edge detector is applied on the RGB-red plane. The outcome often contains many circles of similar radii, which have to be eliminated to the single circle matching the fisheye circle boundary.

The second step uses the color image converted to a grayscale image. It is then converted to black and white with an improved intensity and constant threshold. The improved intensity uses a spread of the normalized histogram, where the grayscale values of the image from 0.25 to 0.75 are expanded to the full range of 0 to 1. It improves the reliability of images with sun reflections on the lens case, which could otherwise be detected as a wrong boundary. The threshold value used to convert the grayscale image to black and white was obtained by trial and error. The threshold used for this application was in the range of 0.2 to 0.4 (on a 0 to 1 scale), depending on the illumination of the image sequences.

The result from this second step and the Canny operation show the fisheye circle boundary. The last step removes the unwanted image parts, as it was illustrated in Figure 8. The resulting black and white image, which contains only one circle shaped edge, is used for the Hough Transform presented in the next section.

3.3 Vibration Estimation using Hough Transform

Since images from a fisheye lens provide a circle-like visible feature, it is possible to estimate a vibration of the lens using the Hough Transform. The vibration estimation presented in this section tracks the movement of the circle center over sequences of images.

Most of the fisheye images are likely to be within a certain range of vibration, which was previously defined to be ±10 pixels in x- and y-direction at 1 pixel increments. Further, the radius is assumed to stay within ±10 pixels range at 0.5 pixels increments. These assumptions considerably reduce the computational complexity of the Hough Transform.

The implementation follows the well known Hough Transform for circles, within defined ranges, as [8]. A circle can be described as in equation (1), where (x_m , y_m) is the center and r the radius of the circle.

$$r^2 = (x - x_m)^2 + (y - y_m)^2 \qquad (1)$$

The algorithm is speed optimized, using MATLAB's matrices calculation features, by solving equation (1) with matrices as in Figure 9. However, the computational complexity of a Hough Transform using 3 parameters (in case of a circle) is known to exceed desktop PC capabilities by using a significant amount of memory (>10GB of RAM), to store the large matrices. The algorithm is therefore optimized to test only for possible circles within the ranges stated in the previous section. This reduces the computational complexity and allows processing within seconds on a desktop PC.

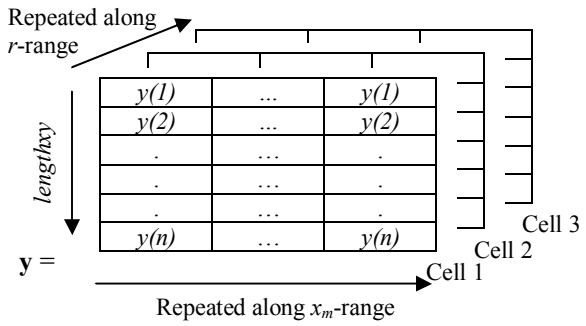

Figure 9: Example of building the 3 dimensional input matrix

The parameters known (or with a known range) are x, y, r and x_m. The parameters x and y contain the coordinates for each detected, estimated circle point in the black and white image and are of length *lengthxy*. The radius r and one of the center coordinates (x_m or y_m) are set to be within the discussed ranges.

The Hough Space (accumulator array) contains the solution for the best matching circle and its center coordinates (x_m , y_m). However, there are some issues to select the correct radius, as discussed in the next section. To find the best matching radius, the image pixels found by the edge detection are compared with each radius. This is implemented as an AND operation of two images, one containing the selected pixels by the edge detection and one containing the pixels striped by the circle. The sum of remaining pixels in the resulting image gives a magnitude of matching pixels for the specific circle (center location and radius). The more matching pixels we have, the higher the probability of a correct radius.

The differences of these coordinates and the estimated positions from the calibration give the estimated translational shift of the fisheye image, due to the vibration. The fisheye lens distortion function (Gurtner et al. [1]) has to be shifted by this amount to compensate for the errors introduced by the vibration.

The following section presents the results achieved with this vibration compensation.

4. Experimental Results

The resulting Hough Space from section 3.3 can be imagined as a set of overlaid images (called cells), with each cell containing a possible solution. The cell containing the maximum peak value is the matching circle, with its correspondent radius and center coordinates (x_m, y_m).

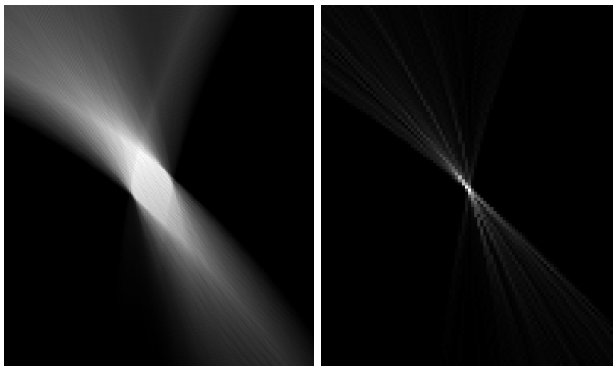

Figure 10: Hough Spaces for all tested radii (left) and for a single radius (right)

However, in practice, multiple possible circles or circles with different radii but similar maxima are found. Figure 11 shows the distribution of matches per radius (solid line) over a range of radii. The maxima are reached around *r=430*, but it shows multiple close matches between *r=420* to *440*. There is no clear separation of the matching radius visible, due to strong

noise on the signal, introduced from a non-circular fisheye boundary detection or misleading pixels. This noise can also be visualized by accumulating each Hough Space cell to a single cell, as shown in Figure 10.

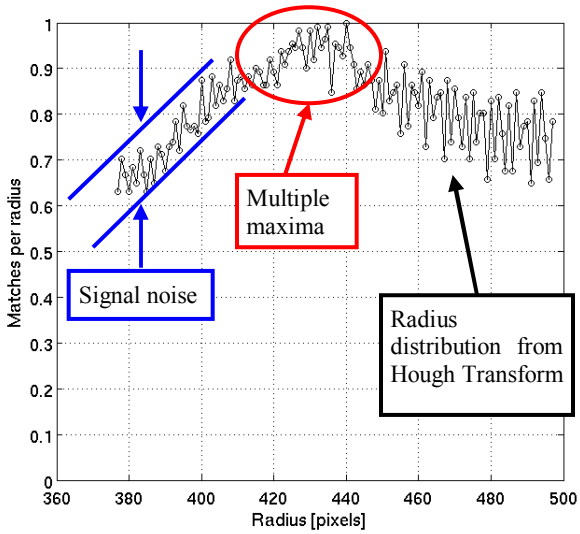

Figure 11: Radius distribution from Hough Transform

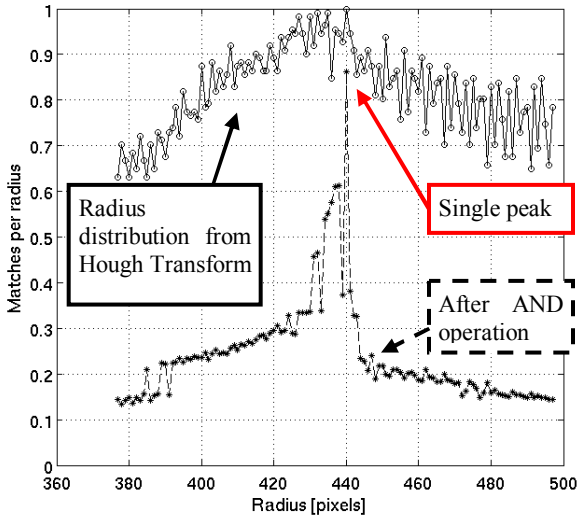

Figure 12: Radius distribution (solid line) and matches after AND operation (dashed line)

As Ryde [10] already mentioned, further processing to interpret the Hough Transform is required, as it was presented in section 3. By applying this AND operation for each cell of the Hough Space, an identifiable separation of one peak (radius) becomes visible (dashed line in Figure 12).

5. Discussion

As we mentioned before, an interpretation of the results from the Hough Transform is essential. This discussion depicts, where the implemented algorithm compensates for the vibrations. Further, the performance and limitations of the presented implementation are discussed.

5.1 Performance

Taking an image sequence and adjusting the algorithm to the current illumination (mainly by adjusting the gray-scale to black and white threshold), the vibration compensation produces clear separated results in >80% of the images, as shown in Figure 12, where the peak is outstanding. In the remaining 20%, it is a double peak in 60% and an unclear result in 40%. However, double peaks are always next to each other, as shown in Figure 13, and can be taken to be the average value of the available resolution. In this case, the compensation works in 92% of the cases.

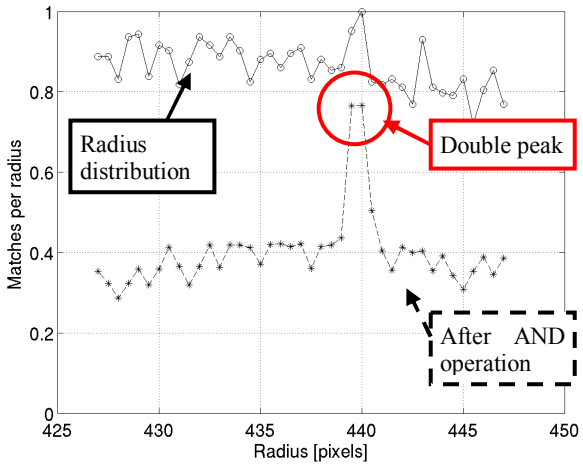

Figure 13: Illustration of a double peak

However, the same threshold used in image sequences, that were flown in the opposite direction (notice the change in illumination) performed much worse (<50% clear hits). By manually adjusting the threshold for this new sequence, the performance raises to the same level.

Another important measurement is the accuracy of the compensation. The vibration was measured in 4 sequences of 20 images manually and compared with the results from the vibration compensation. The compensation achieves in >75% of cases a match within 1 pixel resolution. It must be mentioned that errors can also be introduced from the manual measurement.

It shows to be feasibly to use the Hough Transform in this application, which takes less than 3 seconds of the entire process of 25 seconds per image (Desktop PC, Intel P4, 3.2 GHz).

5.2 Limitations

As have already been stated in the previous section, the current implementation is sensitive to major changes in the illumination, such as flying in the opposite direction or the flying from over land to over water.

Further, the ground truth to proof the compensation results isn't available. A manual method was used to observe the correlation, but introduces new errors as well.

6. Conclusion

This paper presented a new approach to compensate for lens vibrations. The method used in this paper is exclusive for fisheye and similar lenses only (i. e. catadioptric cameras), which show circle-like shapes within the images. The implemented solution with the Hough Transform was shown to be effective and relatively fast in compensating for vibrations in fisheye lens images.

However, there are remaining issues, where the circle boundary merges with the horizon or expanded radius by sun glare causes faulty boundary detections. Further improvement could be gained using more adaptive edge detection methods. Future work includes a statistical approach to find the correct center coordinates and radius or a Hough Transform for ellipse detection to further improve the robustness and selection of the correct circle matching the fisheye circle boundary.

7. Acknowledgements

The authors would like to thank Duncan Greer and Reece Clothier for their contribution for this research at the Australian Research Centre for Aerospace Automation (ARCAA (www.arcaa.com.au)).

8. References

[1] A. Gurtner, W. Boles, and R. Walker, "A Performance Evaluation of Using Fisheye Lenses in Low-Altitude UAV Applications," presented at Second Australasian Unmanned Air Vehicles Conference, AIAC 2007, 2007.

[2] S. Erturk, "Digital image stabilization with sub-image phase correlation based global motion estimation," *Consumer Electronics, IEEE Transactions on*, vol. 49, pp. 1320-1325, 2003.

[3] M. Ramachandran and R. Chellappa, "Stabilization and Mosaicing of Airborne Videos," presented at Image Processing, 2006 IEEE International Conference on, 2006.

[4] G. M. Schuster and A. K. Katsaggelos, "Robust circle detection using a weighted MSE estimator," presented at Image Processing, 2004. ICIP '04. 2004 International Conference on, 2004.

[5] J. C. Russ, *The image processing handbook*, 4th ed. ed. Boca Raton, FL :: CRC Press,, 2002.

[6] R. C. Gonzalez and R. E. Woods, *Digital image processing*, 2nd ed. ed. Upper Saddle River, N.J. :: Prentice Hall,, 2002.

[7] B. Jähne, *Digital image processing*, 5th rev and extended ed. ed. Berlin ; London :: Springer,, 2002.

[8] D. J. Kerbyson and T. J. Atherton, "Circle detection using Hough transform filters," presented at Image Processing and its Applications, 1995., Fifth International Conference on, 1995.

[9] M. C. Shin, D. B. Goldgof, K. W. Bowyer, and S. Nikiforou, "Comparison of edge detection algorithms using a structure from motion task," *Systems, Man and Cybernetics, Part B, IEEE Transactions on*, vol. 31, pp. 589-601, 2001.

[10] J. Ryde and H. Hu, "Fast Circular Landmark Detection for Cooperative Localisation and Mapping," presented at Robotics and Automation, 2005. ICRA 2005. Proceedings of the 2005 IEEE International Conference on, 2005.